When the strategies for cellular selectivity fail. Challenges and surprises in the design and application of fluorescent benzothiadiazole derivatives for mitochondrial staining

Article (Accepted Version)

When the Strategies for Cellular Selectivity Fail. Challenges and Surprises in the Design and Application of Fluorescent Benzothiadiazole Derivatives for Mitochondrial Staining

Pedro H. P. R. Carvalho,[a,b] Jose R. Correa,[a] Karen L. R. Paiva,[a] Michele Baril,[b] Daniel F. S. Machado,[a] Jackson D. Scholten,[b] Paulo E. N. de Souza,[c] Fabiane H. Veiga-Souza,[d] John Spencer,[e] and Brenno A. D. Neto,[a,b]*

[a] Laboratory of Medicinal and Technological Chemistry, University of Brasília, Chemistry Institute (IQ-UnB), Campus Universitário Darcy Ribeiro, Brasília, Distrito Federal, 70904-970, Brazil.

[b] Laboratory of Molecular Catalysis, Institute of Chemistry, Graduate Program (PPGQ), Universidade Federal do Rio Grande do Sul, Porto Alegre, RS, 91501-970, Brazil.

[c] Laboratory of Software and Instrumentation in Applied Physics and Laboratory of Electron Paramagnetic Resonance, Institute of Physics, Campus Universitário Darcy Ribeiro, Brasília, Distrito Federal, 70904-970, Brazil.

[d] Laboratory of Protein Chemistry and Biochemistry, Institute of Biological Sciences, Campus Universitário Darcy Ribeiro, Brasília, Distrito Federal, 70904-970, Brazil.

[e] Department of Chemistry, University of Sussex, Falmer, Brighton, BN1 9QJ, U.K.

Abstract. This work describes a series of fluorescent 2,1,3-benzothiadiazole derivatives (neutral, singly-charged and doubly-charged) to act as bioprobes for mitochondria. The results showed the flaws in the molecular architecture of this class of fluorophores and our attempts to direct the synthesized derivatives to the organelle. Unexpected results also showed a need for new strategies to predict the cellular selectivity of these derivatives. One of the singly-charged derivatives could stain mitochondria selectively whereas the doubly-charged stained the plasma membrane in an unexpected but highly selective manner. Co-staining experiments confirmed the cellular localization of the new derivatives. EPR experiments demonstrated the fluorescent marker that is selective for mitochondria does not interfere in the ROS production of the cells.

Keywords. Benzothiadiazole, mitochondria, plasma membrane, fluorescence, cell-imaging, bioprobe, molecular architecture.

Introduction

The use of fluorescent bioprobes has boosted the knowledge of molecular and cellular biology to a higher level.[1-3] The possibility of selectively monitoring organelle and cellular components with fluorescent small molecules has opened up new perspectives towards the development of medicines and to control specific cellular events.[4-6] Several strategies have been developed during the last decades to improve bioprobe selectivities and stabilities and to overcome several drawbacks such as signal-to-noise ratio, fade off, blinking and membrane permeability.[7-9]

Despite the huge progress observed in the field of bioimaging using molecular bioprobes, there is still much room for improvements and creative applications of both new strategies and new fluorophores.[10] Most state-of-the-art fluorophores are based on a molecular architecture comprising classic scaffolds such as coumarins, boron-dipyrromethenes, fluoresceins, rhodamines, cyanines, and phenoxazines.[11-13] These fluorophores have, however, already shown limitations and drawbacks associated with their use. In this sense, several groups are developing new bioprobes derived from other heterocyclics (Figure 1) such as phenazines,[14] quinolines,[15] pyridines,[16] imidazolones,[17] indoles,[18] pyrimidines,[19] benzothiadiazoles[20] and others.[21-30]

A significant challenge pertains to the appropriate design of stable and efficient fluorophores capable of specific responses inside the astonishing and multifactorial environment of living cells. For some, the ability to transpose the cellular membrane is among the most desirable feature of a fluorogenic probe.[10] Whether capable of transposing the cells' membranes, the probe should specifically stain an organelle or cell component without altering the cellular homeostasis and without interfering in the cells' normal function.

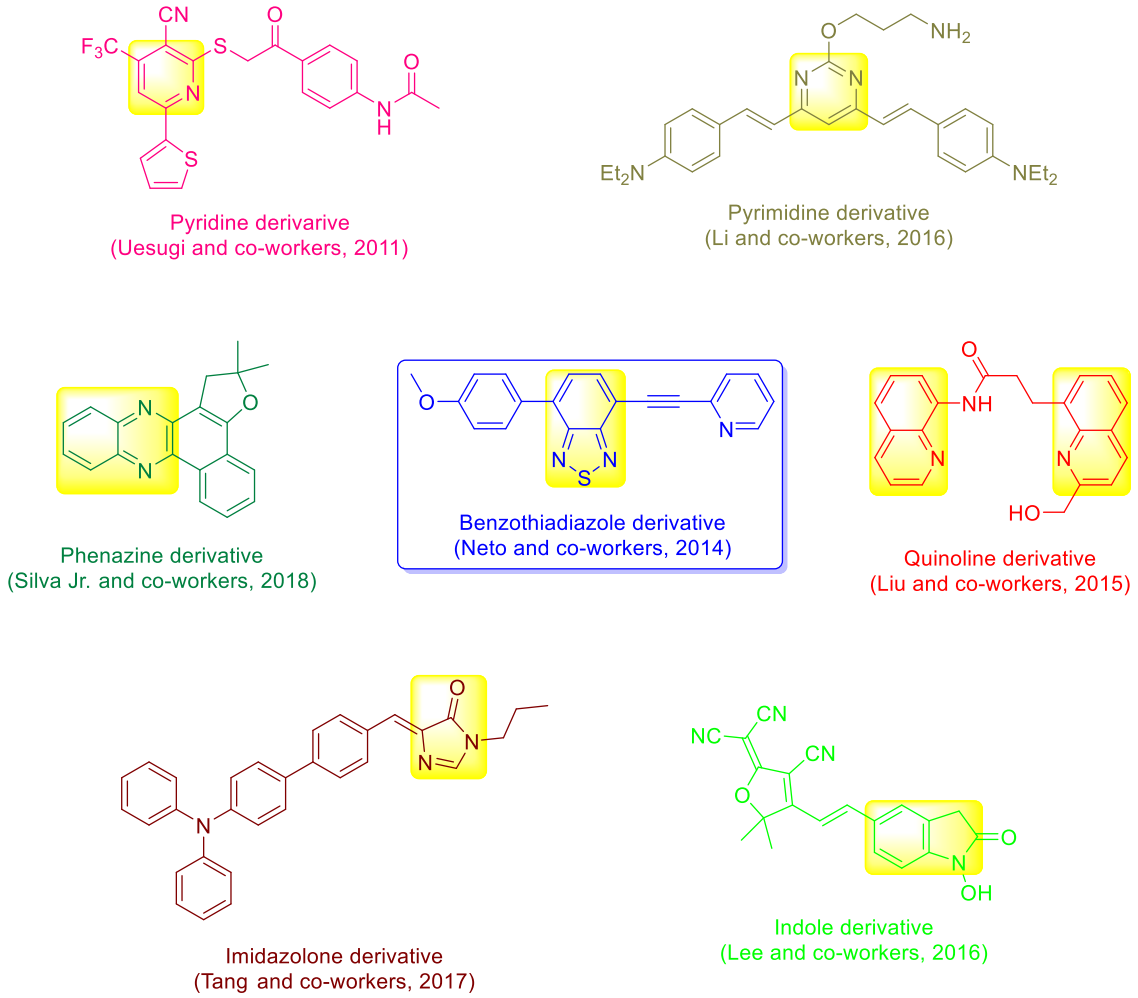

Figure 1. Examples of fluorescent small organic molecules structures based on non-classical heterocyclic scaffolds.

Mitochondria are among the most important organelles, often referred to as "*the guardian of the gate between life and death*".[31] The complexity of mitochondria and their functions in cell regulation[32] render these organelles as outstanding targets to be studied by using fluorescent selective cell markers,[33-35] as highlighted elsewhere.[36] Although there are a few commercial probes to stain mitochondria, their limitations are well documented.[37] For instance, reactive oxygen species (ROS) imbalances may be a consequence of specific mitochondrial labelling by a new fluorophore, but this issue is not addressed when a new mitochondrial marker is published, unless the bioprobe is developed to detect ROS, as described in several and recent examples.[38-48]

We have already disclosed some mitochondrial markers such as fluorescent peptoids,[49] lapachone-based structures,[50] Goniothalamin derivative,[51] multicomponent adducts[52] and benzothiadiazole derivatives.[53] 2,1,3-Benzothiadiazole (BTD) is a new class of fluorescent cell markers, as we have disclosed elsewhere.[54] This heterocyclic has several attractive photophysical properties[55-57] and is typically very stable upon light excitation, as noted in several works.[58-87] After our pioneering works using π-extended BTDs as cellular markers,[54] several groups published fluorescent BTD derivatives for different organelles and cells' components selective staining with success.[88-99]

Despite the many strides in the development of new and selective BTD markers, there still remains much work to be done. For instance, it is necessary to study the commonly used strategies to direct fluorophores inside living cells to a specific organelle using fluorescent BTDs. Some strategies to target mitochondria with organelle-specific fluorophores have been reviewed elsewhere.[100-103] The application of such principles, as in the use of a triphenylphosphonium (TPP) cation usually is a good alternative, as shown in many available reports.[104-106] Indeed, the use of TPP cation allows several molecules and molecular systems to reach the mitochondrial machinery, as recently reviewed.[107] Another attractive idea is the use of charged lipophilic derivatives (typically cations) rather than TPP ions aiming at taking advantage of the highly negative membrane potential of the mitochondrial membrane (≈ -180 mV).[36]

Due to our interest and ongoing efforts to develop the chemistry of selective fluorescent BTDs,[54] we disclose herein a series of fluorescent BTD derivatives and their different cellular responses inside living and fixed cells using the logical chemical synthesis and based on the commonly used strategies to targeting mitochondria with these fluorophores.

Results and Discussion

The first description of a fluorescent BTD capable of selectively staining mitochondria was reported by our group in 2012[108] and it was based on the conjugation of the 2-aminopyridine to the BTD core (Figure 2). Later, based on this work[108] and in other work from our group,[20] Hou and co-workers[93] described the use of two 4-aminopyridine BTD-substituted derivatives (mono- and bis-substituted) for cell imaging. The mono-substituted derivative bearing a bromide atom on the other side (7-position) showed a preference for mitochondria (Figure 2) allowing the use of the probe for quantitative intracellular pH imaging.[93] In the current work, we envisaged the use of aminopyridine mono-substituted BTDs to evaluate their cellular response (Figure 2) and the possibility of using singly- and doubly-charged lipophilic derivatives based on this primary scaffold aiming at the development of a class of BTD-based mitochondrial markers.

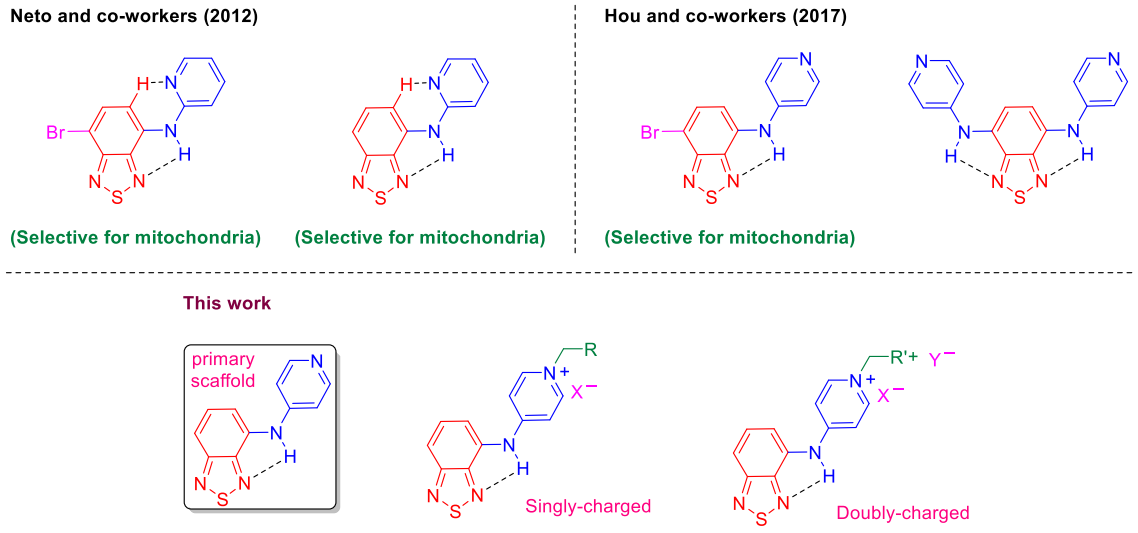

Figure 2. Fluorescent BTDs bearing the aminopyridine group previously described by us,[108] by others[93] and the molecular architecture evaluated in the current work. Note the possibility of singly- and doubly-charged lipophilic cations beyond the neutral primary scaffold based on the incorporation of the 4-aminopyridine group to the BTD core.

The new derivatives were synthesized as shown in Scheme 1. The Buchwald-Hartwig protocol was used to promote the synthesis of **BTD-4AP** (85%) starting from the commercially available **BTD-Br**. **BTD-4AP** could be directly alkylated affording two singly-charged cationic derivatives i.e. **BTD-4APBu** (50%) and **BTD-4APOc** (60%). The synthesis of doubly-charged lipophilic di-cation **BTD-4APBuP** (27%) was also carried out by directly alkylation to incorporate the TPP group to the structure aiming at directing the new structure to the mitochondria, as will be disclosed in due course.

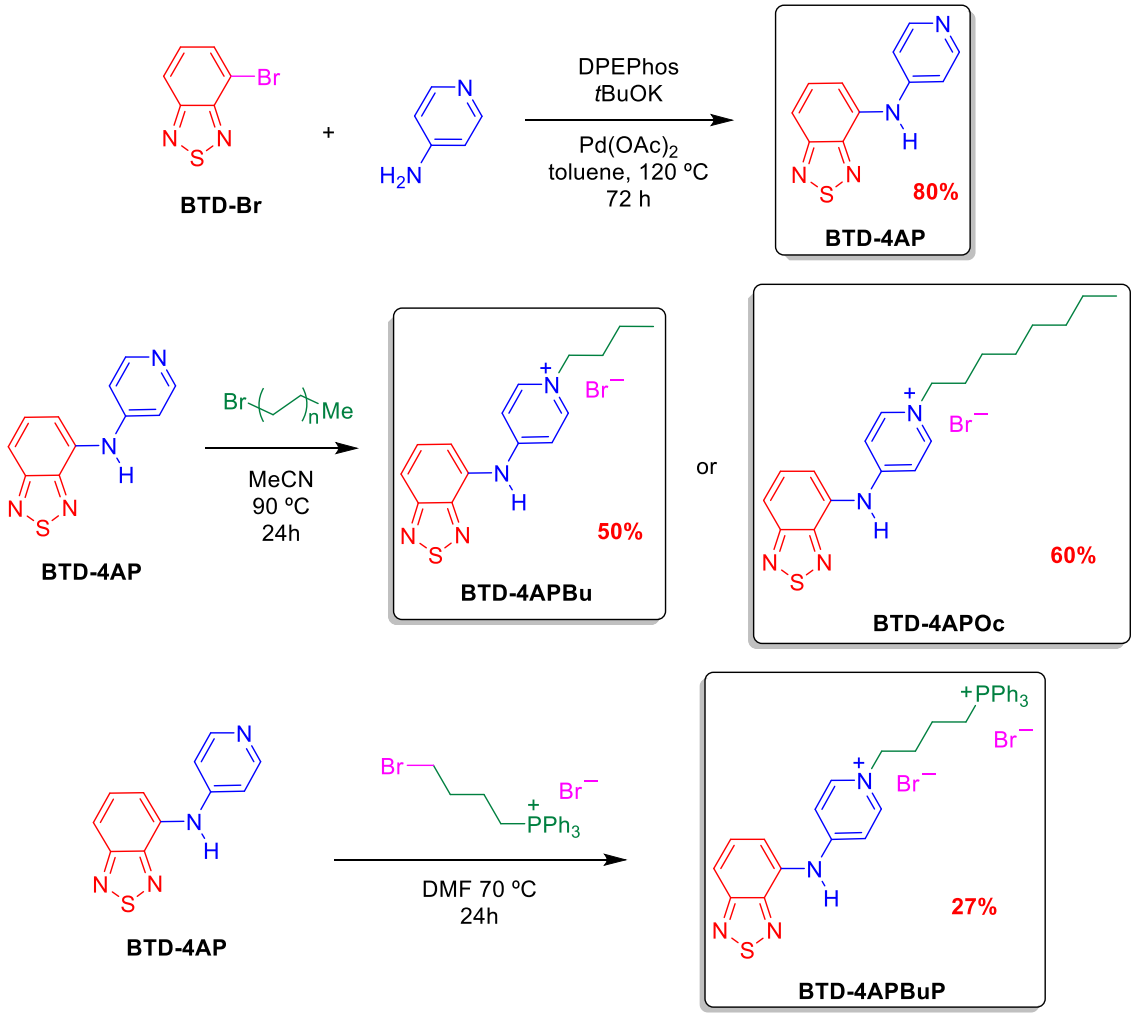

Scheme 1. Synthesis of the fluorescent BTDs derivatives tested in this work.

All compounds were fully characterized (see the Experimental Section for details and the Supporting Information file) and their photophysical properties were evaluated as shown in Figure 3 and Table 1.

Table 1. UV-Vis and fluorescence emission data (in different solvents at 10 μM for all analyses) for the synthesized compounds.

Compound	Solvent	λ_{max}(abs) (nm)	Log ε	λ_{max}(em) (nm)	Stokes Shift (nm / cm^{-1})
BTD-4AP	CH_2Cl_2	404	3.9	543	139 / 6336
	DMSO	417	3.9	570	153 / 6437
	MeCN	403	4.0	551	148 / 6665
	MeOH	402	3.8	572	170 / 7393
	Toluene	404	3.9	533	129 / 5991
	Water	362	3.9	552	190 / 9508
BTD-4APOc	CH_2Cl_2	367	3.4	525	158 / 8200
	DMSO	374	3.5	529	155 / 7834
	MeCN	363	3.3	517	154 / 8206
	MeOH	364	3.3	520	156 / 8242
	Toluene	379	3.4	509	130 / 6739
	Water	366	3.3	552	186 / 9206
BTD-4APBu	CH_2Cl_2	365	3.3	535	170 / 8706
	DMSO	375	3.2	526	151 / 7655
	MeCN	363	3.3	540	177 / 9030
	MeOH	365	3.3	521	156 / 8203
	Toluene	385	2.8	528	143 / 7035
	Water	365	3.2	550	185 / 9215
BTD-4APBuP	CH_2Cl_2	371	3.2	504	133 / 7113
	DMSO	372	2.8	527	155 / 7906
	MeCN	369	3.1	512	143 / 7569
	MeOH	362	3.2	519	157 / 8356
	Toluene	377	2.3	527	150 / 7550
	Water	367	3.2	538	171 / 8661

Quantum yields of fluorescence[109] of the dyes, respectively: 0.27, 0.04, 0.04, 0.01 in MeCN; 0.50, 0.02, 0.01, 0.06 in toluene; 0.001, 0.007, 0.005, 0.050 in water.

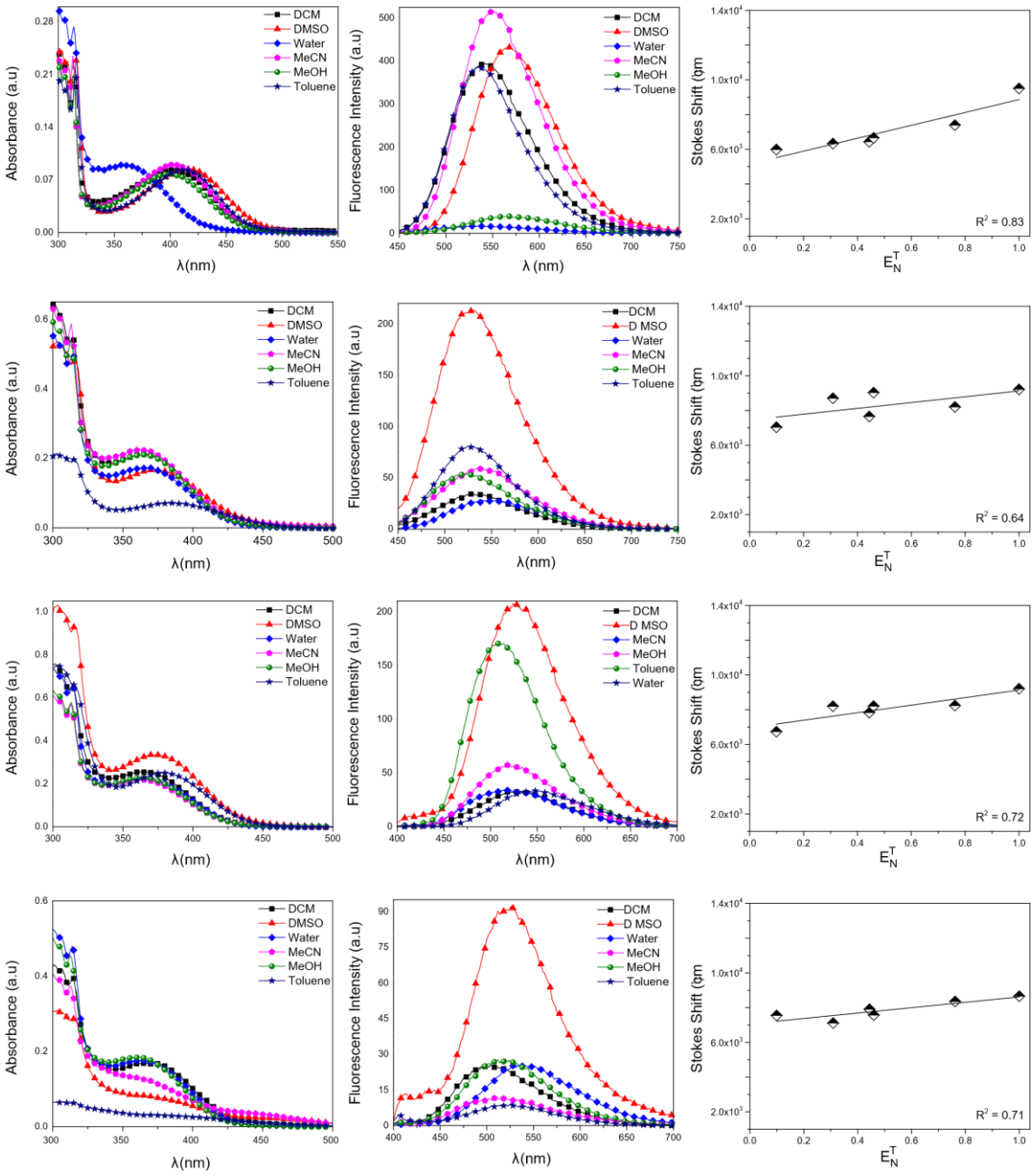

Figure 3. UV-Vis, fluorescence and solvatochromic effect of the synthesized BTDs. From top to bottom: **BTD-4AP**, **BTD-4APOc**, **BTD-4APBu**, and **BTD-4APBuP**. 10 μM for all analyses.

All BTD derivatives showed large Stoke shifts (133-190 nm) indicating their good stability to emit from the first excited-state trough intramolecular charge-transfer (ICT) processes. The relatively large R^2 values of the solvatochromic effect (ETN vs cm^{-1}) plotted using the values provided by Reichardt[110] indicate efficient ICT stabilizing processes taking place from the first excited-state in accordance with the large Stokes

shifts. The calculated linear correlations from the plots also pointed to a considerable ICT contribution, as the obtained values are in accordance with the proposition of Radhakrishnan and co-workers.[111]

To a better understand of the photophysical properties of the synthesized derivatives, theoretical calculations were performed with fully optimized structure geometries (Figure 4).

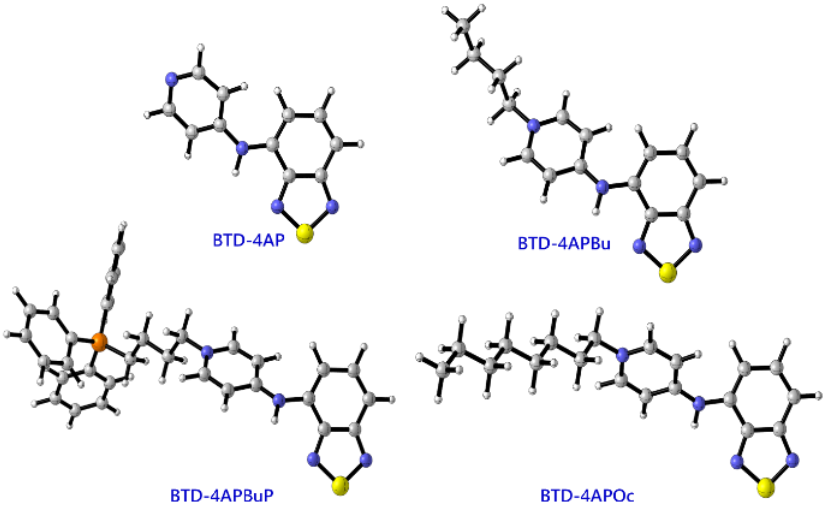

Figure 4. Optimized geometries of **BTD-4AP** (neutral), **BTD-4APBu** (cationic), **BTD-4APBuP** (di-cationic), and **BTD-4APOc** (cationic) in vacuum as obtained at the CAM-B3LYP/6-31G(d) level of theory.

The absorption maxima for the four BTDs in different solvents (PCM) were evaluated from the TD-DFT calculations with different exchange-correlation functionals (XCF) along with the 6-311G+(2d,p) basis set. The performances of the B3LYP, CAM-B3LYP, LC-ωPBE, M06, M062X, and PBE1PBE were assessed to select the most suitable level of theory aiming at describing the electronic optical properties of the fluorogenic dyes. In Table S1 (see the Supporting Information file) it is summarized the calculated absorption maxima for the investigated small-molecules. As expected for this kind of π-extended BTDs,[112-116] the discussion is focused basically on the longest wavelength excitation mode i.e. in characterizing the π-π* transitions.

To obtain a more precise elucidation of the relative performances of the six XCF studied herein, a statistical analysis was performed and it is provided in Figure 5, where it is reported the mean absolute error (MAE) accounting for the maxima absorption peak position associated with the π-π* transitions. LC-ωPBE, and B3LYP to a lesser extent, provided less accurate positions than the other four XCF. As depicted from Figure 5, M06 and PBE1PBE yielded the best overall performance across all studied solvents with absolute deviations below 20 nm, except for the case of **BTD-4AP** although the value is still acceptable, and therefore, these were selected as the "optimal" XCF to be studied in further detail. The relatively poor performance of LC-ωPBE in TD-DFT calculations including solvent effects (PCM) was already reported for other organic chromophores as discussed elsewhere.[117] It turned out that the results obtained using M06 and PBE1PBE were essentially the same, so M06 was not included in the remainder of the discussion, reserving the M06 results to the Supporting Information section.

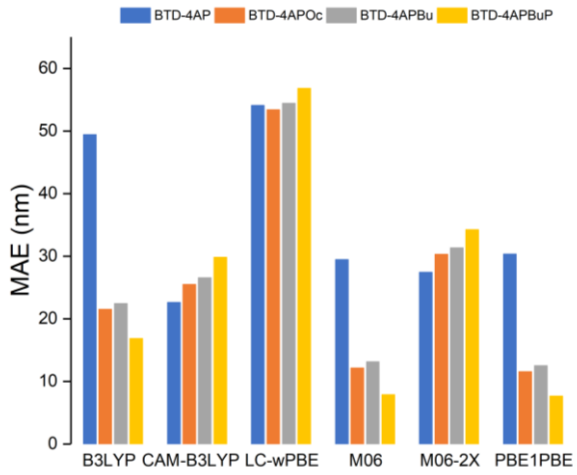

Figure 5. Mean Absolute Error (MAE) comparing both the experimental and the theoretical λ_{max} positions in different solvents for all BTDs studied herein. The computed λ_{max} corresponds to the largest wavelength band associated to the $S_0 \rightarrow S_1$ electronic excitations. All theoretical calculations were performed under the TD-DFT framework using different DFT exchange-correlation functionals along with the People-type basis set 6-311+G(2d,p).

The theoretical absorption spectra of the BTDs calculated at the PBE1PBE/6-311+G(2d,p)//CAM-B3LYP/6-31G(d) level of theory were first determined, as shown in Figure S1 in the Supporting Information. On balance, the simulated absorption spectra exhibited the same behavior of the experimental excitation bands and the following should be considered: (i) the band associated with the longest λ is much less intense when compared with the band associated with the shorter λ. (ii) the PCM solvation scheme did not result in significant solvatochromic shifts, which was also observed in the experimental measurements (Figure 3 and Table 1) where the nature of the solvent did not affect the position of the bands, with some exceptions in the cases of **BTD-4AP** in water and **BTD-4APBu** in toluene. At first glance, the simulated spectra in toluene showed somewhat erratic behavior for the cationic derivatives with the two bands showing a similar pattern. This was however also evident in the experimental measurement of the di-cationic **BTD-4APBuP** in toluene where the two bands exhibited the same intensity.

The molecular orbitals involved in the $S_0 \rightarrow S_1$ electronic excitations associated with the longest wavelength band are displayed in Figure 6 showing that these transitions are basically HOMO-LUMO type bearing strong π-π* character. LUMO orbitals were strictly centered on the BTD core, which is an expected feature owing to the strong electron withdrawing property of this heterocyclic. As shown in Figure 6, the HOMO orbitals do not spread beyond **BTD-4AP** basic scaffold when additional fragments are added to it, especially when **BTD-4APBu** is compared with **BTD-4APOc**, meaning the lengthening of the alkyl chain did not affect the π-π* transitions. These band peaks are basically at the same wavelength since additional sp^3 carbons insert only low energy σ levels (see Figure S2).

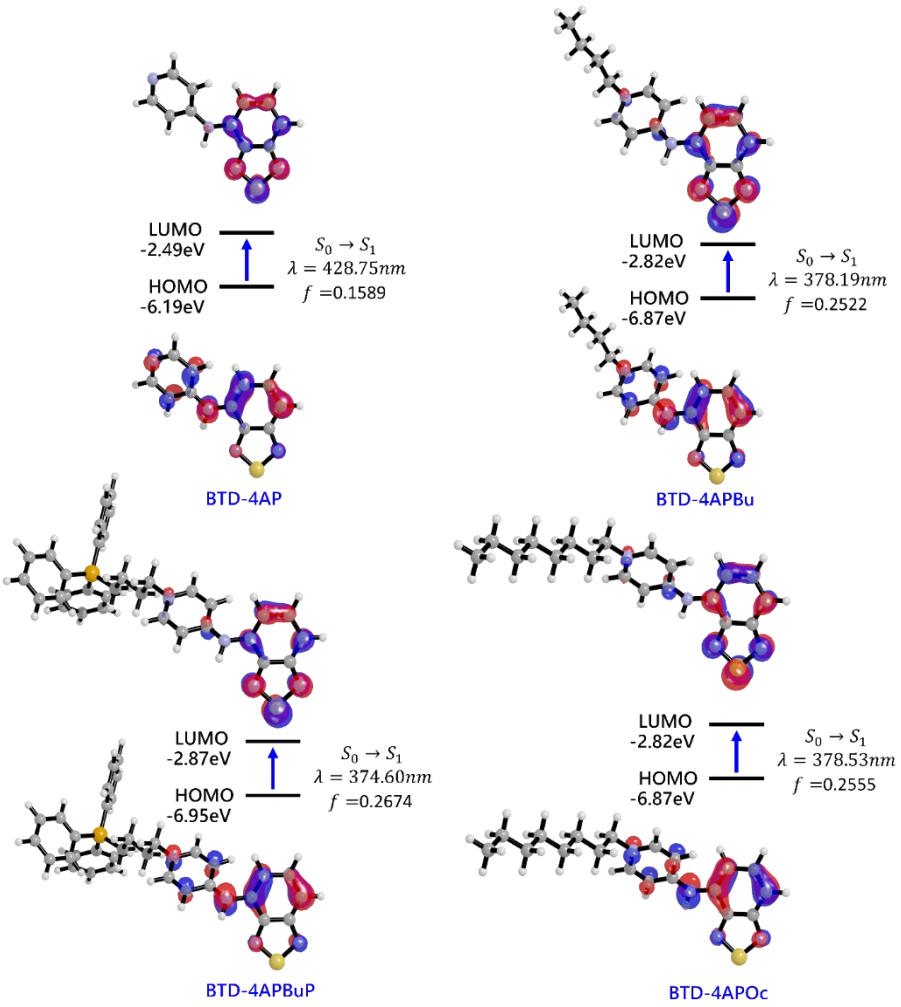

Figure 6. PBE1PBE/6-311+G(2d,p)//CAM-B3LYP/6-31G(d) HOMO and LUMO orbitals of **BTD-4AP**, **BTD-4APBu**, **BTD-4APBuP**, and **BTD-4APOc** in acetonitrile involved in the $S_0 \rightarrow S_1$ electronic excitation associated with the longest wavelength band.

The theoretical results were basically in accordance with the experimental data and all features accounted indicate what the solvatochromic study already indicates i.e. the ICT stabilizing processes from the first excited states are favored for the designed and synthesized structures.

All BTDs were then submitted to MTT tests to evaluate whether these derivatives had cytotoxicity effects or not (Figure S3). At 10 μM of concentration, no cytotoxic effect is noted and it required 100 μM and 24 h to an expressive effect, excepted for **BTD-**

4APOc at 10 μM and only for T47D lineage, but the probes were used much less concentrated than 10 μM. After 24 h of analysis, therefore, no significant cytotoxic effect could be noted for these derivatives at low concentrations, thus indicating they could be evaluated as cell-imaging probes, especially considering the new probes were evaluated at 1 μM.

The new BTD derivatives had then their abilities as bioprobes initially assessed in MCF-7 (breast cancer cells). The initial tested compound i.e. **BTD-4AP** should in principle display a mitochondrial preference (also see Figure 2), but as seen in Figure S4, the dye was found dispersed in the cytosol with no clear preference for any organelle. The same response was obtained by changing the cells' lineages and the fluorophore was again found dispersed in the cytosol for A2780 (human ovarian carcinoma cells, Figure S5), T47D (human breast tumor cells, Figure S6) and HUVEC (human umbilical vein endothelial cells, Figure S7) lineages. The obtained results were highly unexpected considering the presence of a bromine atom at 7-position of the BTD core (see Figure 2), as shown by Hou and co-workers,[93] directs the dye exclusively to the mitochondria. The derivatives of the 2-aminopyridine (with or without a bromine atom as seen in Figure 2), as we demonstrated before,[108] were also found exclusively at the mitochondria. These results indicate how difficult is the task of designing and predicting the cellular preference of a BTD bioprobe.

Aiming for a precise mitochondrial staining, we decided to alkylate the **BTD-4AP** with a *n*-butyl group affording **BTD-4APBu**. This derivative had two features to help towards a mitochondrial selection: (i) it was turned into a cationic dye and therefore prone to use the mitochondrial membrane potential to select this organelle;[101] (ii) the presence of a *n*-butyl group improved the lipophilicity of the dye and this feature may help towards a mitochondrial preference.[100] **BTD-4APBu**, when incubated with the same cells

lineages, returned as the net result a clear preference for selecting mitochondrial in both live and fixed cells (Figures S8-S11). The probe however showed leakage from the organelle being therefore only a reasonable marker, thus avoiding its use as a selective bioprobe to stain mitochondria.

Considering the only possible modification to sustain the basic envisaged scaffold (**BTD-4AP**) was the substituent at the nitrogen of the pyridyl group, and that the use of lipophilic butyl group alongside with the presence of a positive charge seemed to help toward the mitochondrial selection, we decided to use a larger side chain. An *n*-octyl group was therefore incorporated by a direct alkylation of the **BTD-4AP** affording the fluorescent derivative **BTD-4APOc** (see Scheme 1). The new derivative had in principle a more lipophilic character and this feature should assist the probe to reach the mitochondrial machinery with a higher affinity. When tested in live and fixed cells, the **BTD-4APOc** dye proved to be capable of an efficient mitochondrial staining with a bright green emission inside both live and fixed cells (Figure 7).

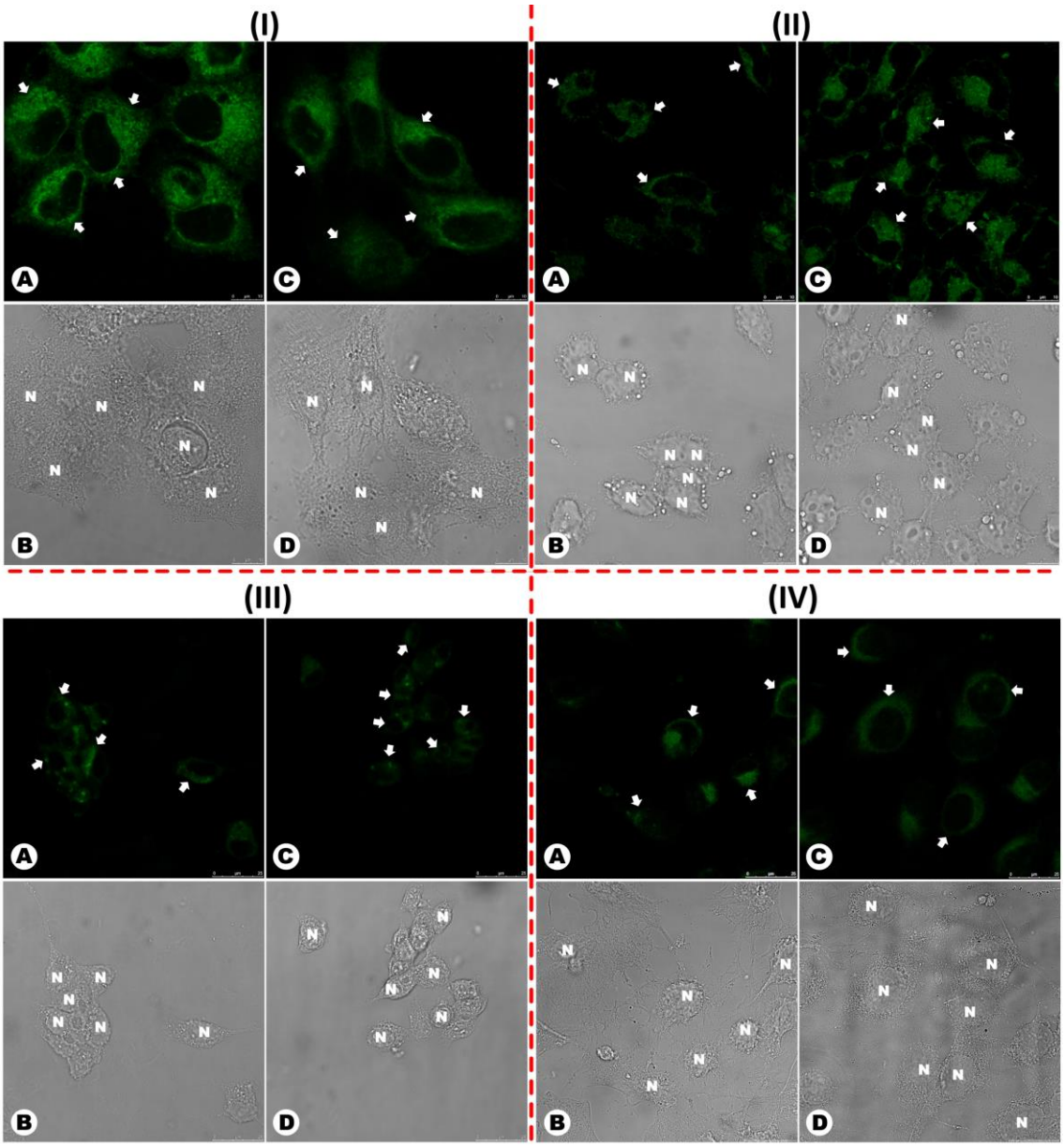

Figure 7. Fluorescent profile of different cells lineages incubated with **BTD-4APOc** (1 μM) in live (A) and (B) and fixed cells (C) and (D). (I) MCF-7, (II) A2780, (III) T47D and (IV) HUVEC cells lineages. (A) and (C) Show the staining distribution obtained with of **BTD-4APOc** in cells cytoplasm with accumulation in the regions near to the nuclei, as indicated to white arrows (mitochondria). Note the accumulation in the cytoplasm (white arrows) in a region near to the cells' nuclei in both samples, known to be rich in mitochondria. The nuclei in these images are represented by black voids indicated by the letter N. (B) and (D) Show the normal morphological aspects of the samples by phase contrast microscopy. Scale bar of 10 μm.

To an additional confirmation of the mitochondrial staining of the developed dye **BTD-4APOc**, co-staining experiments were conducted using the commercially available MitoTracker Red and the results are shown in Figure 8.

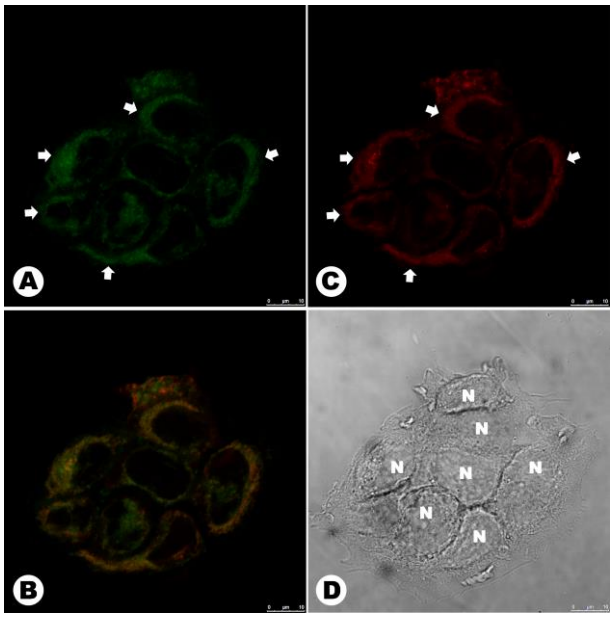

Figure 8. Co-staining experiment using MitoTracker Red (red emission) and **BTD-4APOc** (green emission) in live MCF-7 cells. (A) Mitochondria stained with **BTD-4APOc**. (B) Overlay of (A) and (C) showing the yellow to orange emission as the result of green plus red. (C) Mitochondria stained with MitoTracker Red. (D) Shows the normal morphology of the cells by phase contrast microscopy. The letter N indicates the nuclei of the cells. Scale bar of 10 μm.

It was also performed a quantitative analysis using the Pearson's correlation coefficient (PCC)[118-120] between the two fluorescent signals, that is, the green emission from **BTD-4APOc** and the red emission from MitoTracker. Figure S15 summarizes this find. Data were obtained from ten independent analysis of ten different images. The quantitative results by PCC strong corroborate with the qualitative analysis (Figure 8), therefore showing the distribution within the cells (inside of mitochondria) are noted for both dyes. The negative control were performed using **BTD-4APOc** 90°

counterclockwise rotation and provides additional evidence that none random colocalization had occurred (See Figure S15).

The live cells could be stained selectively with both markers localized at the mitochondria. The fixed cells, however, could not be co-localized because the commercially available MitoTracker Red is known to be dependent on the membrane potential of the organelle to be used as a selective mitochondrial fluorescent dye. According to the manufacturer, this compound is suitable only to stain live cells because of its dependency on the mitochondria membrane potential to work. MitoTracker dyes are cationic fluorophores that accumulate electrophoretically into the mitochondria as a response to the highly negative mitochondrial membrane potential. MitoTracker dyes also possess a reactive chloromethyl group that affords a covalent bond with thiols of proteins and peptides, trapping therefore MitoTracker dyes within the mitochondria. In this sense, when the experiment is performed with fixed cells (Figure 9), no fluorescence is noted with the known commercial dye, but in the meantime an intense green fluorescence is observed when the developed dye is tested. These results show the new **BTD-4APOc** is not dependent on the mitochondrial membrane potential to select this important organelle, being therefore a huge advantage over the available and most used marker.

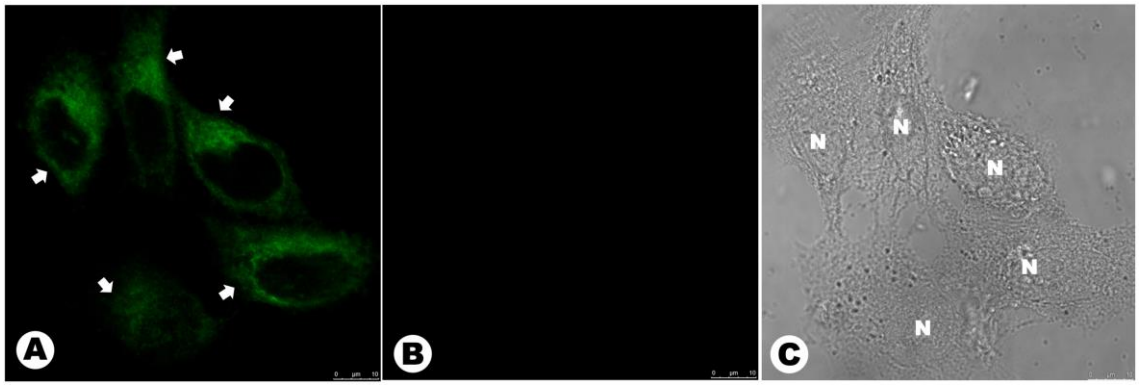

Figure 9. Co-staining experiment using MitoTracker Red (red emitter) and **BTD-4APOc** (green emitter) in fixed MCF-7 cells. (A) Mitochondrial selective staining of fixed cells with **BTD-4APOc**. (B) Fixed cells stained with MitoTracker Red. No fluorescence is noted because the dye is dependent on the membrane potential of the organelles. (C) Shows the normal morphology of the cells by phase contrast microscopy. The letter N indicates the nuclei of the cells. Scale bar of 10 μm.

We also decided to evaluate the strategy of incorporating the TPP group in the structure of **BTD-4APBu** to improve its selectivity towards mitochondria, that is, to evaluate the classical strategy to direct a fluorogenic dye to the mitochondrial structure. As shown in Scheme 1, **BTD-4APBuP** was obtained straight from **BTD-4AP** and the 4-carbons side chain was maintained in the structure of the doubly-charged fluorogenic dye. The fluorophore was then assessed in MCF-7 cells and the results are visualized in Figure 10.

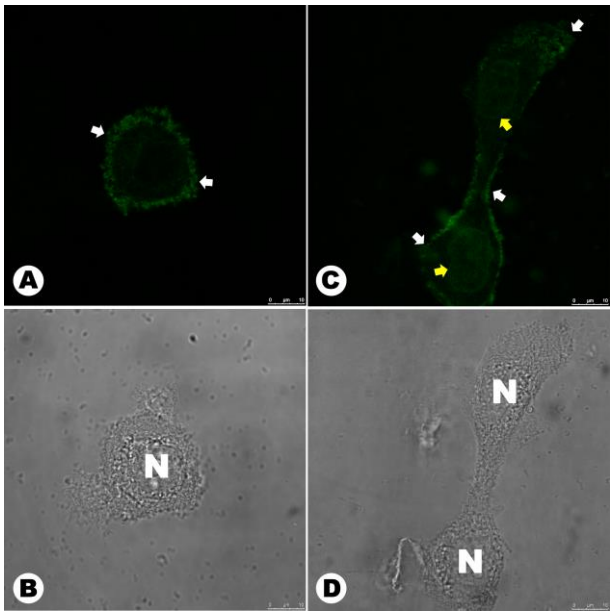

Figure 10. Fluorescent profile of MCF-7 cells lineage incubated with **BTD-4APBuP** (1 μM) in live (A) and (B) and fixed cells (C) and (D). (A) and (C) Show the staining distribution obtained with of **BTD-4APBuP** in the plasma membrane of the cells. The nuclei in these images are represented by black voids indicated by the letter N. (B) and (D) Show the normal morphological aspects of the samples by phase contrast microscopy. The dye was found accumulated in the peripheral region of the cellular membrane (white arrows) in both samples. The nuclear membranes in fixed samples (C) were slight stained (yellow arrows). Scale bar of 10 μm.

The results obtained in the tests of **BTD-4APBuP** were highly unexpected. The probe bearing the TPP group should display a clear preference for mitochondria, but the probe was found in the plasma membrane exclusively. The latter is responsible for the boundary of the cells and the events such as cellular division, endocytosis, exocytosis, apoptosis and signal transduction are associated with this specific and complex cellular structure.[121] The development of plasma membrane-selective probes is a huge challenge[122, 123] and few molecular probes fulfill the requirements to be used as selective bioprobes for this task.[124-126] Although it was designed in principle to stain mitochondria, the surprising results obtained for **BTD-4APBuP** were excellent. In Figure 10-C, tumor cells in the final cytokinesis step are observed, during cellular division with the plasma

membrane clearly delineated by the green emission of the new BTD. Although there is no doubt regarding the selectivity of the bioprobe, confirmatory experiments using the commercially available plasma membrane marker known as CellMask were conducted (Figure 11). The cell membrane specific marker was then tested in different cell lineages with similar results, as seen in Figures S12-S14.

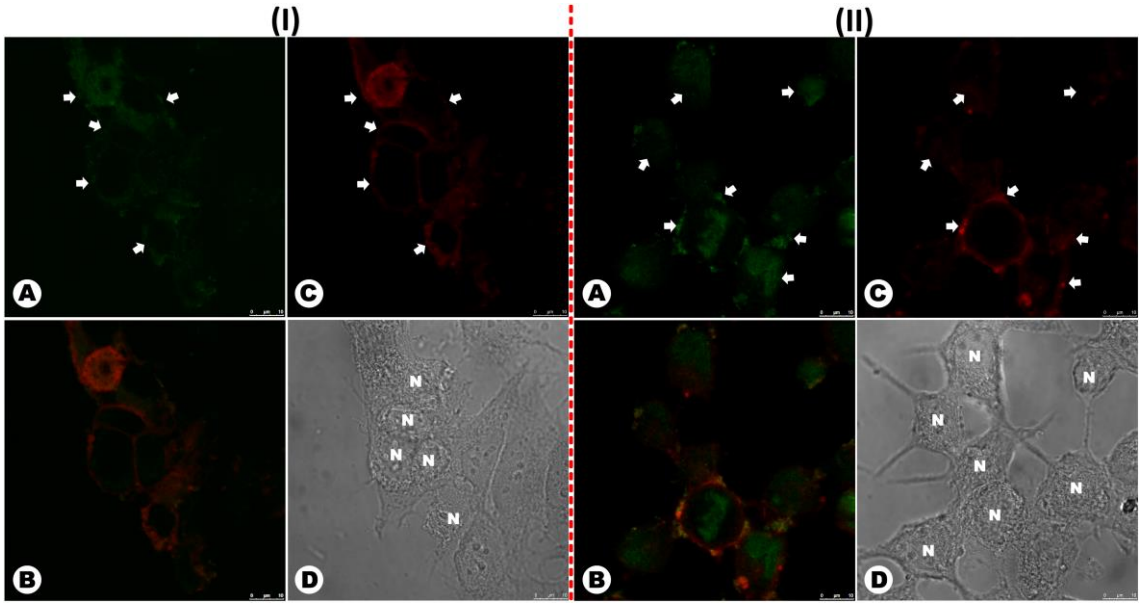

Figure 11. Co-staining experiment using the commercially available CellMask (red emission) and **BTD-4APBuP** (green emission) in (I) live and (II) fixed MCF-7 cells. (A) Plasma membrane stained with **BTD-4APBuP**. (B) Overlay of (A) and (C) showing the yellow to orange emission as the result of green plus red. (C) Plasma membrane stained with CellMask. (D) Shows the normal morphology of the cells by phase contrast microscopy. Arrows indicate the peripherical accumulation of the dyes in the plasma membrane. Note that in (II) the nuclear membrane is also stained by both dyes. The letter N indicates the nuclei of the cells. Scale bar of 10 μm.

In fixed cells (Figure 11-II), the nuclear membranes were also found stained with both dyes. The fixative procedures with formalin compromise the membrane integrity turning the plasma membrane permeable for both the developed dye (**BTD-4APBuP**) and CellMask. These two dyes have affinity for the nuclear membrane, which may be stained only when fixed cells are used, as shown in Figure 11.

Quantitative analyses by PCC were once more performed for both live and fixed cells (Figures S16 and S17, respectively). A PCC of 0.87 was obtained for the live cells and of 0.75 for the fixed cells. As expected, the fixed cells had a slighter lower PCC value as a consequence of membrane integrity loss as a consequence of fixative procedures.

Finally, electron paramagnetic resonance (EPR) experiments were performed to evaluate the influence of the selective mitochondrial marker (**BTD-4APOc**) over the ROS production of the cells. EPR is currently used to a precise determination of intracellular ROS content.[127] To quantify the ROS production, EPR was combined with the spin probe CMH (1-hydroxy-3-methoxycarbonyl-2,2,5,5-tetramethyl-pyrrolidine), which reacts rapidly with the cellular ROS and affords detectable nitroxide radical (CM$^{\bullet}$). The ROS content is quantified by the CMH oxidation, which affords the EPR detectable nitroxide radical (CM$^{\bullet}$) bearing a half-life of h.[128] The following analyses were therefore carried out: (i) negative control experiments to determine the cellular basal level of ROS (with no ROS induction), (ii) analyses in the presence of *N*-acetylcysteine for cellular ROS inhibition, (iii) with menadione for inducing the cellular ROS generation and, at last, (iv) in the presence of **BTD-4APOc** (10 and 100 μM) to compare the effect of the probe in the cellular ROS disbalance. Results are visualized in Figure 12 and Figure S18. To avoid any possible fast reaction and allowing a more precise ROS quantification, all EPR experiments were carried out at liquid nitrogen temperature.

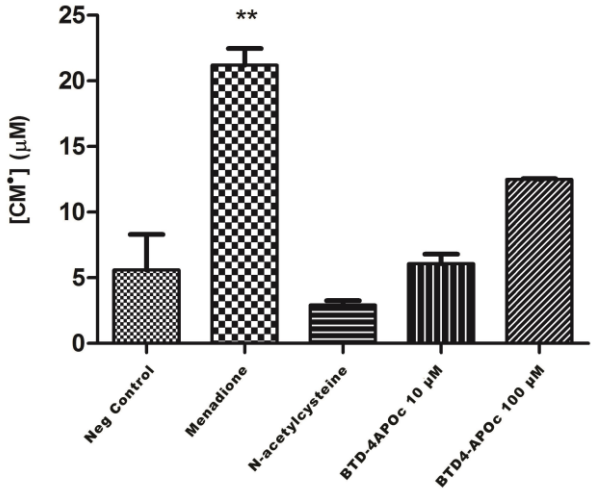

Figure 12. Effects of menadione, *N*-acetylcysteine (NAC) or **BTD-4ApOc** treatments on CM• formation in tumor cells. A higher CM• formation was observed in MCF-7 cells ($p < 0.01$) for menadione treatment only. **$p < 0.01$ compared to control group; one-way ANOVA, followed by Tukey's multiple comparison test.

As depicted in Figure 12, only the known ROS inductor menadione caused a significant ROS alteration in MCF-7 cells. At 10 μM, **BTD-4APOc** did not induced any significant ROS alteration and could be compared with the basal cellular level (negative control). At 100 μM, a small ROS alteration was noted but by far smaller than that observed for menadione induction, that is, the only statistically significant alteration induced by menadione. *N*-Acetylcysteine (NAC) caused a small ROS reduction, as expected for this compound.[129] These results showed the new probe has no effect over the cellular normal function and homeostasis, thus rendering this probe as an outstanding mitochondrial marker.

Conclusions

In summary, a series of new fluorescent BTDs derivatives could be synthesized and applied as live cell-imaging probes. Their molecular architecture was designed to stain mitochondrial selectively, but the results described herein evidenced we are still at the

crawling stage in the science of predicting the relation between the molecular architecture fluorescent BTDs and their cellular responses. **BTD-4AP** showed a diffuse cytosol staining and could not be used to stain mitochondria at all, although the available evidence pointed firmly to this response. The classical strategy to induce mitochondrial selection, that is, the incorporation of TPP group in the fluorophore structure failed and the designed probe (**BTD-4APBuP**) proved to have a high and unexpected affinity for the plasma membrane. The other designed probe for mitochondrial selective staining (**BTD-4APBu**) showed a reasonable staining, but a clear leakage was noted and this feature does not allow its use as selective mitochondrial bioprobe. The molecular architecture of **BTD-4APBu** associated with the cellular result allowed the development of a highly selective mitochondrial marker named **BTD-4APOc**, which not only stained mitochondrial in live and fixed cells, but it was also innocent on the ROS production at the organelle, as demonstrated by EPR experiments. **BTD-4APOc** did not alter the cellular basal ROS level neither interfered at the cellular homeostasis. Although we and other groups (see cited references) have already described huge advances on the use of fluorescent BTDs as selective cellular bioprobes, there are still much room for improvements, especially in the design and prediction of new molecular architecture aiming at selective staining inside the astonishing cellular world.

Experimental section

See the Experimental Section details in the Supporting Information File

Supporting Information

NMR, cited figures (bioimaging and others) related with this manuscript are found in the supplementary material. Energies and Cartesian coordinates for all calculated structures cited in this manuscript.

Acknowledgments

This work has been supported by CAPES, CNPq, FINEP-MCT, FAPERGS, FINATEC, FAPDF, and DPP-UnB. BAD Neto also thanks INCT-Transcend group and LNLS. PPGQ-UFRGS is greatly acknowledge by BADN.

References and Notes

There are no conflicts to declare.

1. W. Chyan and R. T. Raines, *ACS Chem. Biol.*, 2018, **13**, 1810-1823.
2. I. Martinic, S. V. Eliseeva and S. Petoud, *J. Lumin.*, 2017, **189**, 19-43.
3. Y. L. Pak, K. M. K. Swamy and J. Yoon, *Sensors*, 2015, **15**, 24374-24396.
4. J. N. Liu, W. B. Bu and J. L. Shi, *Chem. Rev.*, 2017, **117**, 6160-6224.
5. Q. Q. Miao and K. Y. Pu, *Bioconjugate Chem.*, 2016, **27**, 2808-2823.
6. H. Zhu, J. L. Fan, J. J. Du and X. J. Peng, *Acc. Chem. Res.*, 2016, **49**, 2115-2126.
7. Y. H. Tang, D. Y. Lee, J. L. Wang, G. H. Li, J. H. Yu, W. Y. Lin and J. Y. Yoon, *Chem. Soc. Rev.*, 2015, **44**, 5003-5015.
8. L. Levi and T. J. J. Mueller, *Chem. Soc. Rev.*, 2016, **45**, 2825-2846.
9. L. Yuan, W. Y. Lin, K. B. Zheng, L. W. He and W. M. Huang, *Chem. Soc. Rev.*, 2013, **42**, 622-661.
10. A. Nadler and C. Schultz, *Angew. Chem., Int. Ed.*, 2013, **52**, 2408-2410.
11. L. D. Lavis and R. T. Raines, *ACS Chem. Biol.*, 2014, **9**, 855-866.
12. L. D. Lavis and R. T. Raines, *ACS Chem. Biol.*, 2008, **3**, 142-155.
13. N. Johnsson and K. Johnsson, *ACS Chem. Biol.*, 2007, **2**, 31-38.
14. F. de Moliner, A. King, G. G. Dias, G. F. de Lima, C. A. de Simone, E. N. da Silva Junior and M. Vendrell, *Front. Chem.*, 2018, **6**, 339.
15. Z. Shi, Q. Han, L. Yang, H. Yang, X. Tang, W. Dou, Z. Li, Y. Zhang, Y. Shao, L. Guan and W. Liu, *Chem.-Eur. J.*, 2015, **21**, 290-297.
16. Y. Kawazoe, H. Shimogawa, A. Sato and M. Uesugi, *Angew. Chem., Int. Ed.*, 2011, **50**, 5478-5481.
17. M. J. Jiang, X. G. Gu, J. W. Y. Lam, Y. L. Zhang, R. T. K. Kwok, K. S. Wong and B. Z. Tang, *Chem. Sci.*, 2017, **8**, 5440-5446.
18. J. P. Lai, A. Yu, L. T. Yang, Y. X. Zhang, B. P. Shah and K. B. Lee, *Chem.-Eur. J.*, 2016, **22**, 6361-6367.
19. F. Tang, X. Y. Wang, C. Yao, S. Chen and L. D. Li, *RSC Adv.*, 2016, **6**, 77745-77751.
20. P. H. P. R. Carvalho, J. R. Correa, B. C. Guido, C. C. Gatto, H. C. B. De Oliveira, T. A. Soares and B. A. D. Neto, *Chem.-Eur. J.*, 2014, **20**, 15360-15374.
21. A. Goel, S. Umar, P. Nag, A. Sharma, L. Kumar, Shamsuzzama, Z. Hossain, J. R. Gayen and A. Nazir, *Chem. Commun.*, 2015, **51**, 5001-5004.

22. F. Bruyneel, L. D'Auria, O. Payen, P. J. Courtoy and J. Marchand-Brynaert, *ChemBioChem*, 2010, **11**, 1451-1457.
23. B. K. Wagner, H. A. Carrinski, Y. H. Ahn, Y. K. Kim, T. J. Gilbert, D. A. Fomina, S. L. Schreiber, Y. T. Chang and P. A. Clemons, *J. Am. Chem. Soc.*, 2008, **130**, 4208-+.
24. M. Suresh, A. K. Mandal, S. Saha, E. Suresh, A. Mandoli, R. Di Liddo, P. P. Parnigotto and A. Das, *Org. Lett.*, 2010, **12**, 5406-5409.
25. R. C. dos Santos, N. V. D. Faleiro, L. F. Campo, M. L. Scroferneker, V. A. Corbellini, F. S. Rodembusch and V. Stefani, *Tetrahedron Lett.*, 2011, **52**, 3048-3053.
26. R. Bortolozzi, H. Ihmels, L. Thomas, M. Tian and G. Viola, *Chem.-Eur. J.*, 2013, **19**, 8736-8741.
27. S. Feng, Y. K. Kim, S. Yang and Y.-T. Chang, *Chem. Commun.*, 2010, **46**, 436-438.
28. S. Sen, S. Sarkar, B. Chattopadhyay, A. Moirangthem, A. Basu, K. Dhara and P. Chattopadhyay, *Analyst*, 2012, **137**, 3335-3342.
29. Y. Tian, F. Su, W. Weber, V. Nandakumar, B. R. Shumway, Y. Jin, X. Zhou, M. R. Holl, R. H. Johnson and D. R. Meldrum, *Biomaterials*, 2010, **31**, 7411-7422.
30. H. L. Barros, T. Mileski, C. Dillenburg and V. Stefani, *Forensic Chem.*, 2017, **5**, 16-25.
31. C. Cottet-Rousselle, X. Ronot, X. Leverve and J. F. Mayol, *Cytometry Part A*, 2011, **79A**, 405-425.
32. B. C. Dickinson, D. Srikun and C. J. Chang, *Curr. Opin. Chem. Biol.*, 2010, **14**, 50-56.
33. S. O. Raja, G. Sivaraman, A. Mukherjee, C. Duraisamy and A. Gulyani, *Chemistryselect*, 2017, **2**, 4609-4616.
34. O. Sunnapu, N. G. Kotla, B. Maddiboyina, S. Marepally, J. Shanmugapriya, K. Sekar, S. Singaravadivel and G. Sivaraman, *Chemistryselect*, 2017, **2**, 7654-7658.
35. C. S. Abeywickrama, K. J. Wiesinghe, R. V. Stahelin and Y. Pang, *Sens. Actuator B-Chem.*, 2019, **285**, 76-83.
36. A. T. Hoye, J. E. Davoren, P. Wipf, M. P. Fink and V. E. Kagan, *Acc. Chem. Res.*, 2008, **41**, 87-97.
37. J. F. Buckman, H. Hernandez, G. J. Kress, T. V. Votyakova, S. Pal and I. J. Reynolds, *J. Neurosci. Methods*, 2001, **104**, 165-176.
38. S. Maity, S. Das, C. M. Sadlowski, J. T. Zhang, G. K. Vegesna and N. Murthy, *Chem. Commun.*, 2017, **53**, 10184-10187.
39. D. Y. Zhou, O. Y. Juan, Y. Li, W. L. Jiang, T. Yang, Z. M. Yi and C. Y. Li, *Dyes Pigment.*, 2019, **161**, 288-295.
40. Y. J. Gong, M. K. Lv, M. L. Zhang, Z. Z. Kong and G. J. Mao, *Talanta*, 2019, **192**, 128-134.
41. D. W. Li, H. Y. Chen, Z. F. Gan, J. J. Sun, D. Guo and L. L. Qu, *Sens. Actuator B-Chem.*, 2018, **277**, 8-13.
42. S. Leichnitz, J. Heinrich and N. Kulak, *Chem. Commun.*, 2018, **54**, 13411-13414.
43. S. K. Mostakim, S. Banesh, V. Trivedi and S. Biswas, *Inorg. Chem.*, 2018, **57**, 14574-14581.
44. J. L. Han, C. Y. Chu, G. X. Cao, W. X. Mao, S. Wang, Z. Zhao, M. Q. Gao, H. Ye and X. W. Xu, *Bioorg. Chem.*, 2018, **81**, 362-366.
45. L. J. Tang, M. Y. Tian, H. B. Chen, X. M. Yan, K. L. Zhong and Y. J. Bian, *Dyes Pigment.*, 2018, **158**, 482-489.
46. L. Chen, S. J. Park, D. Wu, H. M. Kim and J. Yoon, *Dyes Pigment.*, 2018, **158**, 526-532.
47. A. C. Sedgwick, W. T. Dou, J. B. Jiao, L. L. Wu, G. T. Williams, A. T. A. Jenkins, S. D. Bull, J. L. Sessler, X. P. He and T. D. James, *J. Am. Chem. Soc.*, 2018, **140**, 14267-14271.
48. H. Zhu, Z. Zhang, S. R. Long, J. J. Du, J. L. Fan and X. J. Peng, *Nat. Protoc.*, 2018, **13**, 2348-2361.
49. S. T. A. Passos, J. R. Correa, S. L. M. Soares, W. A. da Silva and B. A. D. Neto, *J. Org. Chem.*, 2016, **81**, 2646-2651.
50. F. S. dos Santos, G. G. Dias, R. P. de Freitas, L. S. Santos, G. F. de Lima, H. A. Duarte, C. A. de Simone, L. M. S. L. Rezende, M. J. X. Vianna, J. R. Correa, B. A. D. Neto and E. N. da Silva Junior, *Eur. J. Org. Chem.*, 2017, 3763-3773.
51. I. Raitz, R. Y. de Souza Filho, L. P. de Andrade, J. R. Correa, B. A. D. Neto and R. A. Pilli, *ACS Omega*, 2017, **2**, 3774-3784.
52. H. G. O. Alvim, J. R. Correa, J. A. F. Assumpcao, W. A. da Silva, M. O. Rodrigues, J. L. de Macedo, M. Fioramonte, F. C. Gozzo, C. C. Gatto and B. A. D. Neto, *J. Org. Chem.*, 2018, **83**, 4044-4053.
53. B. A. D. Neto, J. R. Correa, P. Carvalho, D. Santos, B. C. Guido, C. C. Gatto, H. C. B. de Oliveira, M. Fasciotti, M. N. Eberlin and E. N. da Silva, *J. Braz. Chem. Soc.*, 2012, **23**, 770-781.
54. B. A. D. Neto, P. H. P. R. Carvalho and J. R. Correa, *Acc. Chem. Res.*, 2015, **48**, 1560-1569.
55. Z. X. Peng, Z. B. Wang, Z. W. Huang, S. J. Liu, P. Lu and Y. G. Wang, *J. Mater. Chem. C*, 2018, **6**, 7864-7873.
56. A. Pazini, L. Maqueira, H. C. Avila, F. M. Valente, R. E. Aderne, D. Back, R. Q. Aucelio, M. Cremona and J. Limberger, *Tetrahedron Lett.*, 2018, **59**, 2994-2999.

57. I. Idris, T. Tannoux, F. Derridj, V. Dorcet, J. Boixel, V. Guerchais, J. F. Soule and H. Doucet, *J. Mater. Chem. C*, 2018, **6**, 1731-1737.
58. A. Pathak, K. R. J. Thomas, M. Singh and J.-H. Jou, *J. Org. Chem.*, 2017, **82**, 11512-11523.
59. S. Langis-Barsetti, T. Maris and J. D. Wuest, *J. Org. Chem.*, 2017, **82**, 5034-5045.
60. H. Fang, H. Gao, T. Wang, B. Zhang, W. Xing and X. Cheng, *Dyes Pigment.*, 2017, **147**, 190-198.
61. B. Bardi, C. Dall'Agnese, K. I. M.-C. Ching, A. Painelli and F. Terenziani, *J. Phys. Chem. C*, 2017, **121**, 17466-17478.
62. T. Jadhav, B. Dhokale and R. Misra, *J. Mater. Chem. C*, 2015, **3**, 9063-9068.
63. T. Ishi-i, I. Kitahara, S. Yamada, Y. Sanada, K. Sakurai, A. Tanaka, N. Hasebe, T. Yoshihara and S. Tobita, *Org. Biomol. Chem.*, 2015, **13**, 1818-1828.
64. M. N. K. P. Bolisetty, C.-T. Li, K. R. J. Thomas, G. B. Bodedla and K.-C. Ho, *Tetrahedron*, 2015, **71**, 4203-4212.
65. R. Misra and P. Gautam, *Org. Biomol. Chem.*, 2014, **12**, 5448-5457.
66. K. D. Belfield, M. V. Bondar, S. Yao, I. A. Mikhailov, V. S. Polikanov and O. V. Przhonska, *J. Phys. Chem. C*, 2014, **118**, 13790-13800.
67. Y.-B. Ruan, Y. Yu, C. Li, N. Bogliotti, J. Tang and J. Xie, *Tetrahedron*, 2013, **69**, 4603-4608.
68. A. V. Moro, P. C. Ferreira, P. Migowski, F. S. Rodembusch, J. Dupont and D. S. Ludtke, *Tetrahedron*, 2013, **69**, 201-206.
69. R. Misra, P. Gautam and S. M. Mobin, *J. Org. Chem.*, 2013, **78**, 12440-12452.
70. R. Misra, P. Gautam, T. Jadhav and S. M. Mobin, *J. Org. Chem.*, 2013, **78**, 4940-4948.
71. T. Ishi-i, M. Sakai and C. Shinoda, *Tetrahedron*, 2013, **69**, 9475-9480.
72. S. H. Chen, Z. H. Qin, T. F. Liu, X. Z. Wu, Y. J. Li, H. B. Liu, Y. L. Song and Y. L. Li, *Phys. Chem. Chem. Phys.*, 2013, **15**, 12660-12666.
73. Y. C. Wang, J. Huang, H. Zhou, G. H. Ma, S. X. Qian and X. H. Zhu, *Dyes Pigment.*, 2012, **92**, 573-579.
74. S. Uchiyama, K. Kimura, C. Gota, K. Okabe, K. Kawamoto, N. Inada, T. Yoshihara and S. Tobita, *Chem.-Eur. J.*, 2012, **18**, 9552-9563.
75. D. G. Patel, F. D. Feng, Y. Y. Ohnishi, K. A. Abboud, S. Hirata, K. S. Schanze and J. R. Reynolds, *J. Am. Chem. Soc.*, 2012, **134**, 2599-2612.
76. P. A. Netz, *Int. J. Quantum Chem.*, 2012, **112**, 3296-3302.
77. M. S. Miranda, M. A. R. Matos, V. M. F. Morais and J. F. Liebman, *J. Chem. Thermodyn.*, 2012, **50**, 30-36.
78. L. Y. Lin, C. H. Tsai, F. Lin, T. W. Huang, S. H. Chou, C. C. Wu and K. T. Wong, *Tetrahedron*, 2012, **68**, 7509-7516.
79. F. Garo and R. Haner, *Eur. J. Org. Chem.*, 2012, 2801-2808.
80. L. E. Polander, L. Pandey, S. Barlow, P. Tiwari, C. Risko, B. Kippelen, J. L. Bredas and S. R. Marder, *J. Phys. Chem. C*, 2011, **115**, 23149-23163.
81. D. H. Lee, M. J. Lee, H. M. Song, B. J. Song, K. D. Seo, M. Pastore, C. Anselmi, S. Fantacci, F. De Angelis, M. K. Nazeeruddin, M. Graetzel and H. K. Kim, *Dyes Pigment.*, 2011, **91**, 192-198.
82. Y.-J. Cheng, C.-H. Chen, Y.-J. Ho, S.-W. Chang, H. A. Witek and C.-S. Hsu, *Org. Lett.*, 2011, **13**, 5484-5487.
83. J. L. Wang, Q. Xiao and J. A. Pei, *Org. Lett.*, 2010, **12**, 4164-4167.
84. Y. Li, A. Y. Li, B. X. Li, J. Huang, L. Zhao, B. Z. Wang, J. W. Li, X. H. Zhu, J. B. Peng, Y. Cao, D. G. Ma and J. Roncali, *Org. Lett.*, 2009, **11**, 5318-5321.
85. M. Akhtaruzzaman, N. Kamata, J. Nishida, S. Ando, H. Tada, M. Tomura and Y. Yamashita, *Chem. Commun.*, 2005, 3183-3185.
86. M. Akhtaruzzaman, M. Tomura, J. Nishida and Y. Yamashita, *J. Org. Chem.*, 2004, **69**, 2953-2958.
87. M. Akhtaruzzaman, M. Tomura, M. B. Zaman, J. Nishida and Y. Yamashita, *J. Org. Chem.*, 2002, **67**, 7813-7818.
88. Q. Jiang, Z. Zhang, J. Lu, Y. Huang, Z. Lu, Y. Tan and Q. Jiang, *Bioorg. Med. Chem.*, 2013, **21**, 7735-7741.
89. L. Garcia, M. Lazzaretti, A. Diguet, F. Mussi, F. Bisceglie, J. Xie, G. Pelosi, A. Buschini, D. Baigl and C. Policar, *New J. Chem.*, 2013, **37**, 3030-3034.
90. S. Yao, B. Kim, X. Yue, M. Y. C. Gomez, M. V. Bondar and K. D. Belfield, *ACS Omega*, 2016, **1**, 1149-1156.
91. H. Appelqvist, K. Stranius, K. Borjesson, K. P. R. Nilsson and C. Dyrager, *Bioconjugate Chem.*, 2017, **28**, 1363-1370.
92. D. Yang, H. Wang, C. Sun, H. Zhao, K. Hu, W. Qin, R. Ma, F. Yin, X. Qin, Q. Zhang, Y. Liang and Z. Li, *Chem. Sci.*, 2017, **8**, 6322-6326.

93. X. Han, Z. R. Wang, Q. Cheng, X. R. Meng, D. H. Wei, Y. C. Zheng, J. Ding and H. W. Hou, *Dyes Pigment.*, 2017, **145**, 576-583.
94. C. Dyrager, R. P. Vieira, S. Nystrom, K. P. R. Nilsson and T. Storr, *New J. Chem.*, 2017, **41**, 1566-1573.
95. C. Chen, Y. Hua, Y. Hu, Y. Fang, S. Ji, Z. Yang, C. Ou, D. Kong and D. Ding, *Sci. Rep.*, 2016, **6**, 23190.
96. S. C. Wang, Z. Li, Y. B. Liu, G. Feng, J. Zheng, Z. Yuan and X. J. Zhang, *Sens. Actuator B-Chem.*, 2018, **267**, 403-411.
97. F. Z. Chen, J. Zhang, W. B. Qu, X. X. Zhong, H. Liu, J. Ren, H. P. He, X. H. Zhang and S. F. Wang, *Sens. Actuator B-Chem.*, 2018, **266**, 528-533.
98. J. Y. Sun, P. H. Ling and F. Gao, *Anal. Chem.*, 2017, **89**, 11703-11710.
99. S.-Y. Liou, C.-S. Ke, J.-H. Chen, Y.-W. Luo, S.-Y. Kuo, Y.-H. Chen, C.-C. Fang, C.-Y. Wu, C.-M. Chiang and Y.-H. Chan, *ACS Macro Lett.*, 2016, **5**, 154-157.
100. L. F. Yousif, K. M. Stewart and S. O. Kelley, *ChemBioChem*, 2009, **10**, 1939-1950.
101. B. A. D. Neto, J. R. Correa and R. G. Silva, *RSC Adv.*, 2013, **3**, 5291-5301.
102. Roopa, N. Kumar, V. Bhalla and M. Kumar, *Chem. Commun.*, 2015, **51**, 15614-15628.
103. Z. Xu and L. Xu, *Chem. Commun.*, 2016, **52**, 1094-1119.
104. A. Chakraborty and N. R. Jana, *J. Phys. Chem. C*, 2015, **119**, 2888-2895.
105. H. S. Yuan, H. Cho, H. H. Chen, M. Panagia, D. E. Sosnovik and L. Josephson, *Chem. Commun.*, 2013, **49**, 10361-10363.
106. Z. Hu, Y. Sim, O. L. Kon, W. H. Ng, A. J. M. Ribeiro, M. J. Ramos, P. A. Fernandes, R. Ganguly, B. G. Xing, F. Garcia and E. K. L. Yeow, *Bioconjugate Chem.*, 2017, **28**, 590-599.
107. J. Zielonka, J. Joseph, A. Sikora, M. Hardy, O. Ouari, J. Vasquez-Vivar, G. Cheng, M. Lopez and B. Kalyanaraman, *Chem. Rev.*, 2017, **117**, 10043-10120.
108. B. A. D. Neto, P. H. P. R. Carvalho, D. C. B. D. Santos, C. C. Gatto, L. M. Ramos, N. M. de Vasconcelos, J. R. Corrêa, M. B. Costa, H. C. B. de Oliveira and R. G. Silva, *RSC Adv.*, 2012, **2**, 1524-1532.
109. C. Wuerth, M. Grabolle, J. Pauli, M. Spieles and U. Resch-Genger, *Nat. Protoc.*, 2013, **8**, 1535-1550.
110. C. Reichardt, *Chem. Rev.*, 1994, **94**, 2319-2358.
111. M. Ravi, T. Soujanya, A. Samanta and T. P. Radhakrishnan, *J. Chem. Soc. Faraday Trans.*, 1995, **91**, 2739-2742.
112. D.-C. Lee, Y. Jeong, L. V. Brownell, J. E. Velasco, K. A. Robins and Y. Lee, *RSC Adv.*, 2017, **7**, 24105-24112.
113. D. Jiang, S. Chen, Z. Xue, Y. Li, H. Liu, W. Yang and Y. Li, *Dyes Pigment.*, 2016, **125**, 100-105.
114. T. Jadhav, B. Dhokale, Y. Patil, S. M. Mobin and R. Misra, *J. Phys. Chem. C*, 2016, **120**, 24030-24040.
115. Y. Li, L. Scudiero, T. Ren and W.-J. Dong, *J. Photochem. Photobiol., A*, 2012, **231**, 51-59.
116. W. Zhu, X. Meng, Y. Yang, Q. Zhang, Y. Xie and H. Tian, *Chem.-Eur. J.*, 2010, **16**, 899-906.
117. A. Charaf-Eddin, A. Planchat, B. Mennucci, C. Adamo and D. Jacquemin, *J. Chem. Theory Comput.*, 2013, **9**, 2749-2760.
118. W. Stauffer, H. Sheng and H. N. Lim, *Sci. Rep.*, 2018, **8**, 15764.
119. B. Moser, B. Hochreiter, R. Herbst and J. A. Schmid, *Biotechnol. J.*, 2017, **12**, 1600332.
120. V. Zinchuk, Y. Wu and O. Grossenbacher-Zinchuk, *Sci. Rep.*, 2013, **3**, 1365.
121. H. R. Jia, H. Y. Wang, Z. W. Yu, Z. Chen and F. G. Wu, *Bioconjugate Chem.*, 2016, **27**, 782-789.
122. P. Liu, S. Li, Y. Jin, L. Qian, N. Gao, S. Q. Yao, F. Huang, Q.-H. Xu and Y. Cao, *ACS Appl. Mater. Interfaces*, 2015, **7**, 6754-6763.
123. M. Li, C. Nie, L. Feng, H. Yuan, L. Liu, F. Lv and S. Wang, *Chem.-Asian J.*, 2014, **9**, 3121-3124.
124. R. Kreder, S. Oncul, O. A. Kucherak, K. A. Pyrshev, E. Real, Y. Mely and A. S. Klymchenko, *RSC Adv.*, 2015, **5**, 22899-22905.
125. T. Heek, J. Nikolaus, R. Schwarzer, C. Fasting, P. Welker, K. Licha, A. Herrmann and R. Haag, *Bioconjugate Chem.*, 2013, **24**, 153-158.
126. C. K. Koo, K. L. Wong, C. W. Y. Man, H. L. Tam, S. W. Tsao, K. W. Cheah and M. H. W. Lam, *Inorg. Chem.*, 2009, **48**, 7501-7503.
127. B. R. B. Gomes, M. Firmino, J. S. Jorge, M. L. O. Ferreira, T. M. Rodovalho, S. N. Weis, G. E. P. Souza, P. C. Morais, M. V. Sousa, P. E. N. Souza and F. H. Veiga-Souza, *Free Radic. Res.*, 2018, **52**, 351-361.
128. S. I. Dikalov and D. G. Harrison, *Antioxid. Redox Signal*, 2014, **20**, 372-382.
129. M. Halasi, M. Wang, T. S. Chavan, V. Gaponenko, N. Hay and A. L. Gartel, *Biochem. J.*, 2013, **454**, 201-208.